Optics Communications 281 (2008) 4747–4752

Contents lists available at ScienceDirect

Optics Communications

journal homepage: www.elsevier.com/locate/optcom

Chaotic dynamics of a semiconductor laser with double cavity feedback: Applications to phase shift keying modulation

V.Z. Tronciu [a,b,*], I.V. Ermakov [a,c], Pere Colet [a], Claudio R. Mirasso [a]

[a] Instituto de Física Interdisciplinar y Sistemas Complejos (IFISC) CSIC-UIB, Campus Universitat de les Illes Balears, E- 07122 Palma de Mallorca, Spain
[b] Department of Physics, Technical University of Moldova, Chisinau MD-2004, Republic of Moldova
[c] Optoelectronic devices for research Department, Bauman Moscow State Technical University, Russia

ARTICLE INFO

Article history:
Received 18 March 2008
Received in revised form 23 May 2008
Accepted 25 May 2008

ABSTRACT

We report results on the numerical investigations of the dynamical behavior of a single mode semiconductor laser under the influence of double cavity optical feedback. We find that the system displays, under certain conditions, chaotic behaviors appropriate for chaos based communications. The synchronization of two unidirectional coupled (master–slave) systems is also studied. The influence of some parameters on the resynchronization and autocorrelation times is investigated. We find that the resynchronization time for the proposed scheme can be two orders of magnitude shorter when compared with that of the single-cavity feedback case. Very good conditions for message encoding by using the on/off phase shift keying encryption method are identified and examples of message encoding/decoding are presented.

1. Introduction

During recent years the phenomenon of synchronization has received considerable attention in many research areas [1]. In particular chaotic waveforms have found applications in chaos based communication systems. Although the technique was originally proposed in electronic circuits [2,3] it has strongly developed in optical systems where different setups for chaotic data transmission have been proposed [4,5]. From the application point of view, chaos based communications has become an option to improve privacy and security in data transmission, especially after the recent field demonstration on the metropolitan fiber networks of Athens [6]. In optical chaos based communications the chaotic waveform is usually generated by using semiconductor lasers subject to either all-optical [7–11] or electro-optical [12–14] feedback. In particular, semiconductor lasers subject to the influence of all-optical feedback from a distant mirror have been investigated extensively for the past two decades and different dynamical behaviors have been characterized, including periodic and quasi-periodic pulsations, low frequency fluctuations and coherence collapse (for more details see Ref. [15]). Integrated lasers with ultrashort feedback cavities have also revealed similar characteristics if the feedback is properly amplified [16]. Configurations using Fabry–Perot resonators providing the optical feedback, the so called frequency selective feedback, have also been studied [17–19]. In this case the feedback can either destabilize the laser emission or improve the stability of the CW emission allowing the control of the laser in a non-invasive way [17].

Lasers subject to feedback from two cavities have been considered in several configurations. In particular, feedback from a second cavity has been used to control the chaotic dynamics of semiconductor lasers with optical feedback [20–23] or to hide the information about the delay time [24]. Control in the low frequency fluctuation regime has been achieved by adjusting properly both the length and feedback strength of the second external cavity. Phase locking has also been found in a semiconductor laser with two external cavities. Contrary to these previous studies, we aim in this paper to use a second cavity to generate a high dimensional chaotic waveform and at the same time profit from the second branch for on/off phase shift keying (OOPSK) encryption purposes [25,26]. We anticipate that when using the second branch as a perturbation of the main one we get resynchronization times that are much shorter than those obtained with a single cavity allowing bit rate transmission of hundreds of Mbit/s.

The paper is structured as follows. We start in Section 2 by describing the model for the investigated scheme. Section 3 presents a study of the dynamics of a laser under the influence of a double cavity optical feedback (DCF). In Section 4 we highlight the advantages of the proposed setup when compared with the conventional optical feedback (COF) case and the OOPSK encryption method is demonstrated for the DCF. Finally, the summary and conclusions are given in Section 5.

* Corresponding author. Address: Instituto de Física Interdisciplinar y Sistemas Complejos (IFISC) CSIC-UIB, Campus Universitat de les Illes Balears, E- 07122 Palma de Mallorca, Spain. Tel.: +34 971 171314.
E-mail address: vasile@ifisc.uib.es (V.Z. Tronciu).

0030-4018/$ - see front matter © 2008 Elsevier B.V. All rights reserved.
doi:10.1016/j.optcom.2008.05.053

2. Model

The proposed setup is depicted schematically in Fig. 1. It consists of a semiconductor laser coupled to the external reflectors R_1 and R_2, that could be implemented, e.g., by using two fiber cavities. The advantage of the proposed scheme is that we can control two feedback strengths, two feedback phases and two delay times independently. The feedback branch governed by reflectivity R_1 is called conventional feedback branch (CFB) and the one governed by R_2 the modulated feedback branch (MFB). Assuming fiber based cavities with a refractive index of 1.5 we consider the delay time in the CFB to be $\tau_1 = 0.5$ ns and that of MFB $\tau_2 = 0.3$ ns. In the model we only account for single reflexions in both branches. In the absence of coupling, the correlation between the transmitter and receiver outputs is negligible. When a certain amount of light from the transmitter is injected into the receiver, the latter is able to synchronize to the emitter under appropriate conditions. Once synchronized, a message can be encoded into the carrier. At the receiver side, the message can be recovered via the chaos pass filtering process [27]. Several encoding schemes have been proposed in the literature [28,29]. One of the most attractive schemes in terms of security is the OOPSK method [25,26] where the codification is achieved by slightly modulating the phase of the optical feedback of the emitter. The physical basis for OOPSK is that the synchronization behavior of the receiver acts as a sensitive detector for variations of the transmitter feedback phase: suitable discrete changes yield the dynamics of the receiver to jump between synchronized and de-synchronized states. In contrast to these drastic changes in the receiver dynamics changes in the emitter dynamics should not be noticeable neither in the intensity dynamics, nor in the RF or optical spectra. The principle of the ON/OFF phase shift keying encryption works as follows. The message is encoded by switching between two states of the master system that yield highly correlated (synchronized) states (Bit "0") or less correlated (desynchronized) states (Bit "1") in the receiver system. Hence, the message can be simply recovered by monitoring the synchronization error. The controlled variations in the master system can be accomplished by inserting, e.g., an electrooptical modulator within the external cavity of the transmitter. The message is decoded by detecting whether the receiver synchronizes or not with the input carrier [26]. Up to now this technique has the disadvantage that the maximum modulation rate is only of some tens of Mbit/s [25,26,30].

In the present study, the laser dynamics is analyzed in the framework of the extended Lang-Kobayashi equations for the complex field amplitude E and an excess carrier density N [31]

$$\frac{dE_{t,r}}{dt} = (1+i\alpha)\left[\frac{g(N_{t,r}-N_0)}{1+s|E_{t,r}|^2} - \frac{1}{\tau_{ph}}\right]\frac{E_{t,r}}{2} + \gamma_1 e^{i\varphi}E_{t,r}(t-\tau_1) + \gamma_2 e^{i\psi}E_{t,r}(t-\tau_2) + k_r E_t \quad (1)$$

$$\frac{dN_{t,r}}{dt} = \frac{I_{t,r}}{e} - \frac{1}{\tau_e}N_{t,r} - \frac{g(N_{t,r}-N_0)}{1+s|E_{t,r}|^2}|E_{t,r}|^2 \quad (2)$$

The subscripts t and r refer to transmitter and receiver lasers, respectively. The last term in the Eq. (1) is present only in receiver laser and describes the unidirectional coupling between transmitter and receiver. κ_r is the coupling strength given by $\kappa_r = \sqrt{1-R}\eta_{ext}/(\tau_c\sqrt{R})$ where R is facet power reflectivity of the slave laser ($R = 30\%$), τ_c is the cavity roundtrip time of the light within the laser ($\tau_c = 8.5$ ps), η_{ext} accounts for losses different than those introduced by the laser facet ($\eta_{ext} = 0.5$) resulting in $\kappa = 90$ ns^{-1}. τ_1 and τ_2 are roundtrip time in the CFB and MFB, respectively. γ_1 and γ_2 are the feedback strengths governed by the reflectivities R_1 and R_2, respectively. $\phi = \omega_0\tau_1$, and $\psi = \omega_0\tau_2$ are the accumulated optical phases in the CFB and MFB, respectively, which, without loss of generality, can be assumed to take values between 0 and 2π. The other parameter values are: $\alpha = 5$ the linewidth enhancement factor; $g = 1.5\times10^{-5}$ ns^{-1} the differential gain parameter, $s = 4\times10^{-7}$ the gain saturation coefficient, $\tau_{ph} = 2$ ps and $\tau_e = 2.0$ ns the photon and carrier lifetimes, respectively and $N_0 = 1.5\times10^8$ the carrier number at the transparency. These parameters, that are considered identical for both lasers, are used for the calculated results shown in all figures in the paper. The injection current is fixed at $I = 45$ mA ($I_{th} = 14.7$ mA). For the model given by Eq. (1) and (2) if $\tau_1 = \tau_2$ the feedback term in (1) can be reduce to a COF term with an equivalent feedback coefficient given by $\tilde{\gamma}e^{i\tilde{\varphi}} = \gamma_1 e^{i\varphi} + \gamma_2 e^{i\psi}$.

3. Transmitter laser dynamics

In this section we discuss the behavior of a semiconductor laser under the influence of a DCF. For small enough feedback strengths semiconductor lasers under the influence either of COF or DCF show CW or pulsating operations. Chaotic behavior appears if the feedback strength is increased enough. Fig. 2b illustrates typical time traces (left) and the power spectra (right) of a laser under the influence of a DCF operating in a robust chaotic regime. We mention that the behavior shown in Fig. 2a is similar to that of a laser under the influence of COF with $\gamma = 40$ ns^{-1}, $\tau = 0.5$ ns and identical laser parameters. It is well known, that the autocorrelation time is related to the complexity of the generated chaos. The shorter the correlation time is the more chaotic and less predictable the dynamics is. The calculations of the autocorrelation time for the traces shown in Figs. 2a and b [16] yield similar result for both COF and DCF with values of $T_{ac}^{COF} \sim T_{ac}^{DCF} \sim 100$ ps for our parameter values. A confirmation of this property is given below. Fig. 3a shows the autocorrelation time, as a function of feedback strength for COF for $\tau = 0.5$ ns (solid line) and $\tau = 2$ ns (dotted line). It can be clearly seen that as the feedback strength and delay time are increased the autocorrelation time decreases, an indication that the laser dynamics becomes more chaotic. Fig. 3b shows the calculated autocorrelation time for a laser under the influence of DCF. The feedback strength of CFB is fixed to $\gamma_1 = 30$ ns^{-1} while that of MFB is varied. For zero MFB strength the resynchronization and autocorrelation times coincide with that of COF for $\gamma = 30$ ns^{-1}.

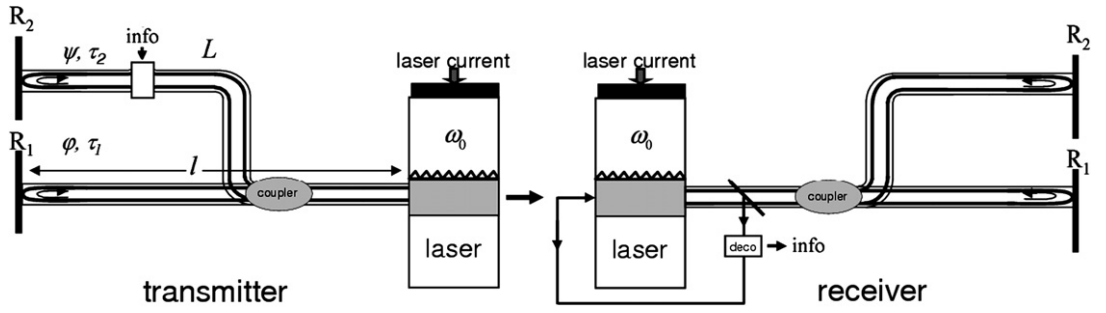

Fig. 1. Investigated setup. A laser with fiber-based external cavities. The cavity lengths are $l = 0.05$ m ($\tau_1 = 0.5$ ns) and $L = 0.03$ m ($\tau_2 = 0.3$ ns). The refractive index of the optical fiber is $n = 1.5$.

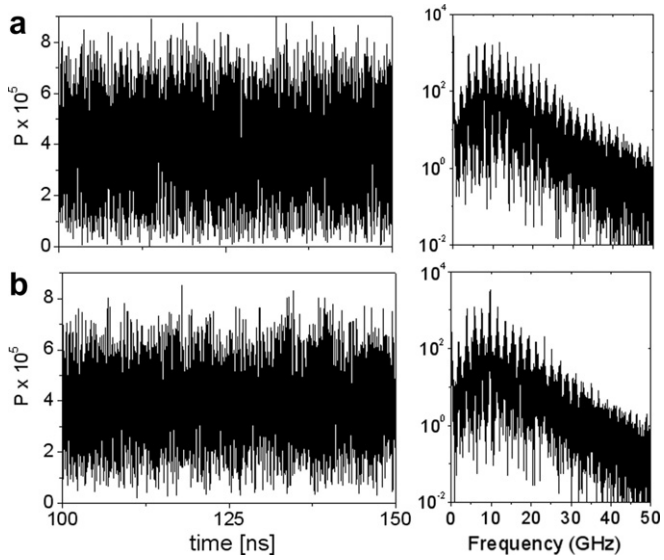

Fig. 2. Time traces of the output power P (left) and the power spectrum (right) for (a) COF for $\gamma = 40\ \mathrm{ns}^{-1}$, $\tau = 0.5$ ns, and $\phi = 0$; and (b) DCF for $\gamma_1 = 30\ \mathrm{ns}^{-1}$, $\gamma_2 = 10\ \mathrm{ns}^{-1}$, $\tau_1 = 0.5$ ns, $\tau_2 = 0.3$ ns, $\phi = 0$, and $\psi = \pi/2$.

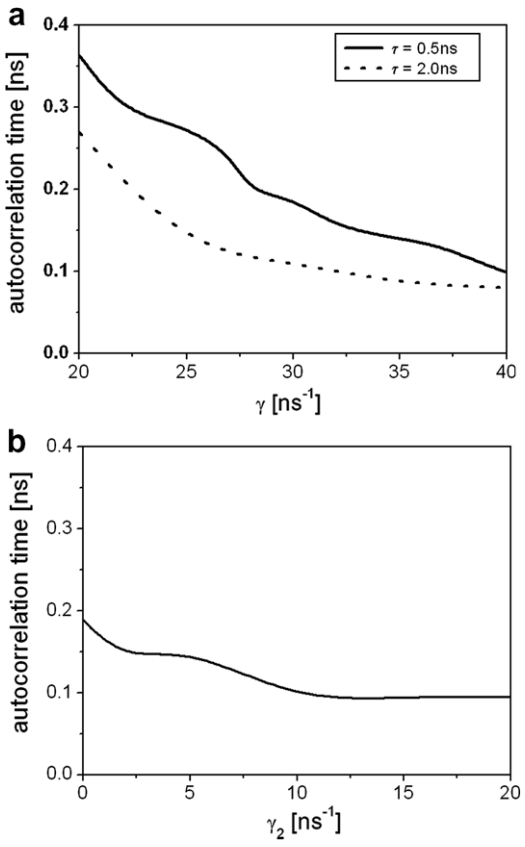

Fig. 3. The autocorrelation time as a function of feedback strength for (a) COF for $\phi = 0$, and different values of delay time, (b) DCF of MFB for $\gamma_1 = 30\ \mathrm{ns}^{-1}$, $\phi = 0$, $\psi = \pi/2$, $\tau_1 = 0.5$ ns, $\tau_2 = 0.3$ ns.

An increase of feedback strength of MFB leads to a decrease of autocorrelation time up to 0.1 ns similar to that of COF. However, when the MFB is introduced the resynchronization time can be expected to become much shorter as a result of only distortion of the chaotic attractor generated by the CFB.

Fig. 4a displays a typical bifurcation diagram of a semiconductor laser under the influence of COF with the feedback strength acting as a bifurcation parameter and $\tau = 0.5$ ns, $\phi = 0$. As the feedback strength is increased several bifurcations take place. For each value of the feedback strength the figure displays the values of the maxima of the time traces of the emitted power. It is well known that as the feedback strength is increased a scenario compatible with quasiperiodic route to chaos appears [15]. Figs. 4b and c display the bifurcation diagrams of a semiconductor laser subject to DCF for the feedback strength and feedback phase acting as bifurcation parameters. Let us, e.g., consider the case of feedback strength for the CFB fixed to $\gamma_1 = 30\ \mathrm{ns}^{-1}$ while the feedback strength of MFB is increased. Considering $\phi = 0$ and $\psi = \pi/2$, as shown in Fig. 4b, even for low values of the feedback strength γ_2 the dynamics of the laser is already chaotic due to the influence of the feedback of CFB. It can be noticed from the figure that the amplitude of the chaotic oscillations slightly increases with the feedback strength γ_2 (see Fig. 4b). When both feedback strengths are fixed to $\gamma_1 = 30\ \mathrm{ns}^{-1}$, $\gamma_2 = 10\ \mathrm{ns}^{-1}$ and the phase $\phi = 0$, as shown in Fig. 4c, fully developed chaotic dynamics is found for any value of MFB phase ψ.

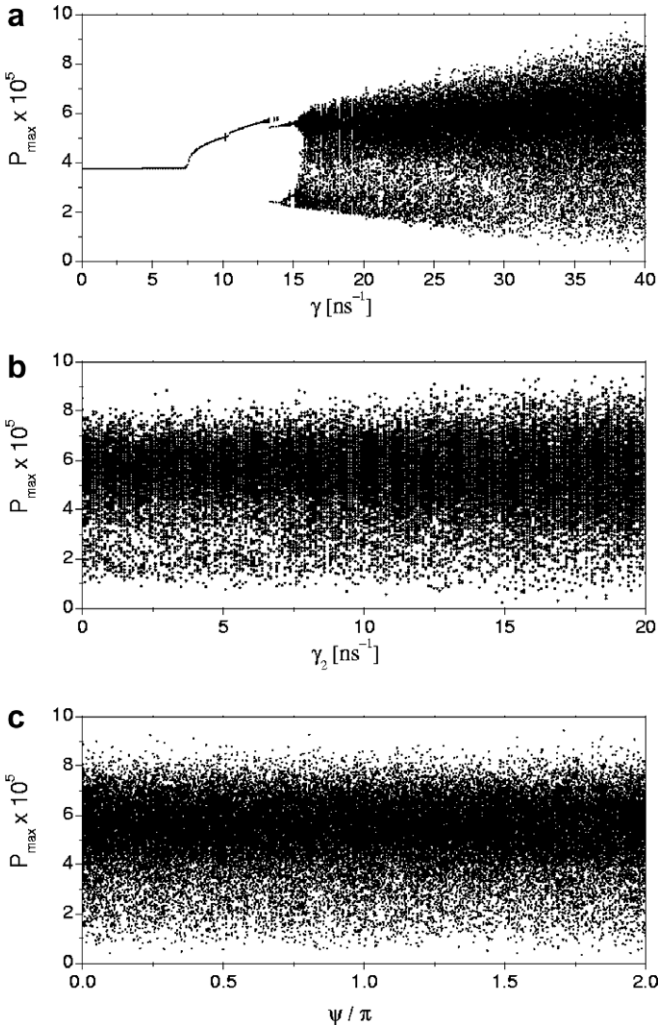

Fig. 4. Bifurcation diagrams of the output power for (a) COF with the feedback strength γ as bifurcation parameter for $\phi = 0$; (b) DCF with γ_2 as bifurcation parameter; $\gamma_1 = 30\ \mathrm{ns}^{-1}$, $\phi = 0$ and $\psi = \pi/2$; (c) DCF with the MFB phase ψ as bifurcation parameter; $\gamma_1 = 30\ \mathrm{ns}^{-1}$, $\gamma_2 = 10\ \mathrm{ns}^{-1}$ and $\phi = 0$. Each dot represents a peak of the output power.

4. Synchronization and message transmission

So far we have clarified different aspects of the transmitter laser dynamics under a DCF. In what follows we focus on the transmitter–receiver configuration and evaluate the synchronization properties. Since our final aim is to use the auxiliary branch to perform OOPSK encryption, it is important to characterize in advance the resynchronization time, i.e., the time required by the setup to synchronize when the link between master and slave lasers is interrupted. The inverse of the resynchronization time is an estimation of the maximum modulation rate that can be achieved with the OOPSK technique. We estimate the resynchronization time as the time needed by the system to achieve a correlation coefficient of 0.98 when starting from an initial uncoupled configuration, for which the correlation between emitter and receiver is close to zero [32]. Fig. 5 shows the resynchronization time as a function of feedback strength for a laser under the influence of COF for different values of delay time τ and different coupling coefficient κ in a region where the system displays a chaotic behavior.

As shown in Fig. 5a for delay time $\tau = 0.5$ ns two regimes are observed. For $\gamma \ll \kappa_r$ the resynchronization time grows linearly with a small slope and it is of the order of a few roundtrip time. When γ becomes larger the resynchronization time grows exponentially. This last regime appears for $\gamma > 27\ \mathrm{ns}^{-1}$ when $\kappa_r = 60\ \mathrm{ns}^{-1}$ and for $\gamma > 33\ \mathrm{ns}^{-1}$ when $\kappa_r = 90\ \mathrm{ns}^{-1}$. The separation in the regimes comes from a competition between the coupling strength κ_r and the feedback strength γ. For $\kappa_r >> \gamma$ the first dominate leading to a small resynchronization time while when both are similar there is a transient competition, which induces large resynchronization time. Finally for $\gamma >> \kappa_r$ no synchronization is observed. Similar behaviour is observed for a large delay time $\tau = 2$ ns (see Fig. 5b), although now the resynchronization time in the first regime grows linearly with a larger slope.

Fig. 6a shows the calculated resynchronization time for a laser under the influence of DCF. The feedback strength of CFB is fixed to $\gamma_1 = 30\ \mathrm{ns}^{-1}$ while that of MFB is varied. For zero MFB feedback strength the resynchronization time coincides with that of COF for $\gamma = 30\ \mathrm{ns}^{-1}$. An increase of the MFB feedback strength up to $\gamma_2 = 20\ \mathrm{ns}^{-1}$, leads only to a smooth increase of the resynchronization time up to a value approximately 7 ns. A first comparison between Figs. 5 and 6 shows evidence that the DCF has some advantages with respect to the COF. When the feedback strength of COF is $40\ \mathrm{ns}^{-1}$, the resynchronization time is approximately 300 ns while for the DCF with $\gamma_1 = 30\ \mathrm{ns}^{-1}$, $\gamma_2 = 10\ \mathrm{ns}^{-1}$ the resynchronization time is approximately 3ns (see Fig. 6a). In fact, we have found that when using the DCF setup we can reduce the resynchronization time by two orders of magnitude when compared with the COF setup. This decrease in the resynchronization time can be attributed to the fact that for low feedback strength

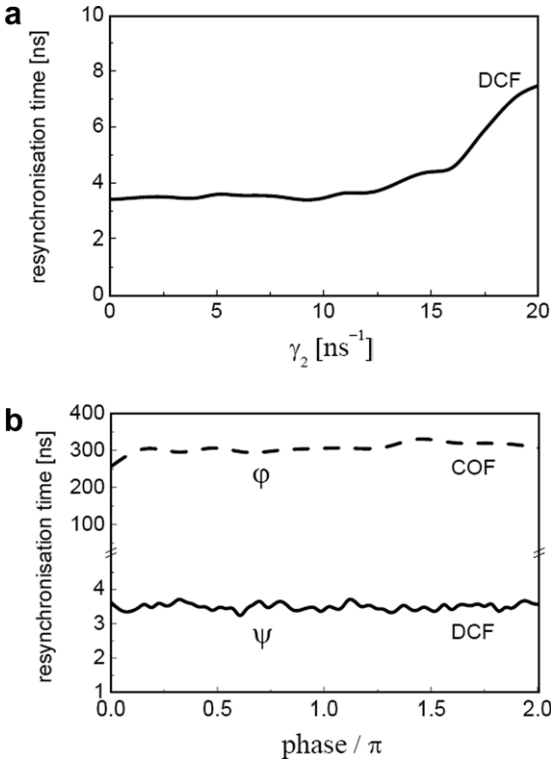

Fig. 6. Resynchronization recovery time as a function of different parameters (a) the feedback strength γ_2 of MFB for DCF for $\gamma_1 = 30\ \mathrm{ns}^{-1}$, $\phi = 0$, $\psi = \pi/2$, (b) the feedback phase for the COF (dashed line) and for the DCF (solid line). The parameters for the COF are $\gamma = 40\ \mathrm{ns}^{-1}$ and $\tau = 0.5$ ns. The parameters for the DCF are $\gamma_1 = 30\ \mathrm{ns}^{-1}$, $\gamma_2 = 10\ \mathrm{ns}^{-1}$, $\phi = 0$, $\tau_1 = 0.5$ ns, $\tau_2 = 0.3$ ns. $\kappa_r = 90\mathrm{ns}^{-1}$.

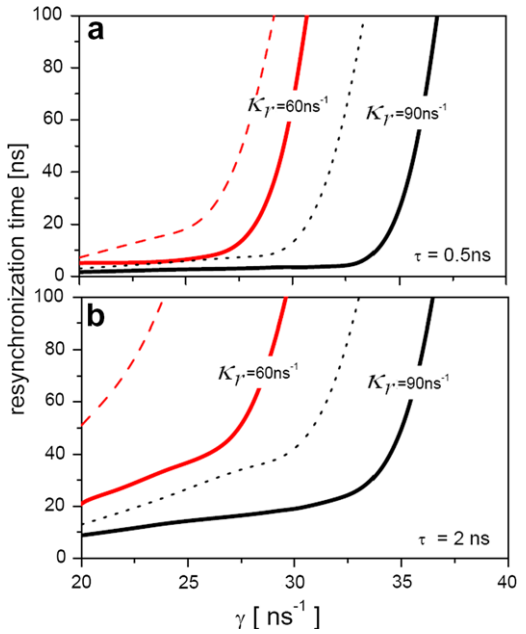

Fig. 5. Resynchronization time as a function of feedback strength for COF for $\phi = 0$ and the delay time $\tau = 0.5$ ns (a) and $\tau = 2$ ns (b). Results are obtained from 100 random initial conditions. Thick lines show the average resynchronization time, while thin lines show the maximum value of those 100 realizations.

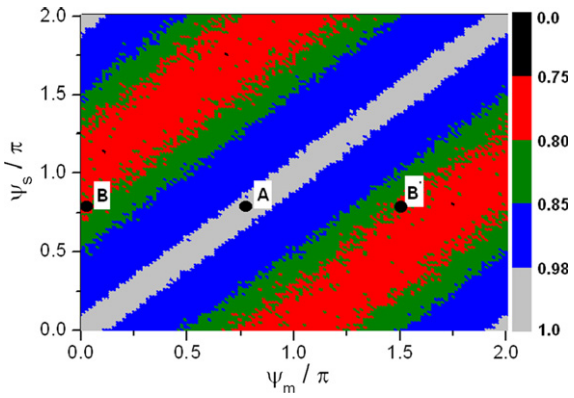

Fig. 7. Cross correlation coefficient in the $\psi_m - \psi_s$ phase space. The other parameters are $\gamma_1 = 30\ \mathrm{ns}^{-1}$, $\gamma_2 = 10\ \mathrm{ns}^{-1}$, $\kappa_r = 90\ \mathrm{ns}^{-1}$, $\phi_m = \phi_S = 0$. A high degree of synchronization is characterized by light grey level. Phases are varied in 0.05 radians steps.

values the MFB acts as a weak perturbation of the strong chaotic attractor generated by the CFB. This fact yields shorter resynchronization times when compared to the COF case. Fig. 6b shows, with solid line, the resynchronization time as a function of MFB phase ψ for DCF, for $\gamma_1 = 30\ \mathrm{ns}^{-1}$, $\gamma_2 = 10\ \mathrm{ns}^{-1}$, $\phi_m = \phi_S = 0$. The dashed line shows the resynchronization time as a function of optical feedback phase of the COF case for $\gamma = 40\ \mathrm{ns}^{-1}$, $\phi = 0$. From these results it can be clearly seen that the DCF system resynchronizes much faster that the COF system for any value of the feedback phase. We have checked that these results also hold for any value of the COF phase ϕ.

Now we consider the influence of a mismatch between the phases ψ of the slave laser with respect to that of the master laser on the cross correlation coefficient. Fig. 7 shows the values of this coefficient in the plane $(\psi_m - \psi_s)$ for feedback strengths $\gamma_1 = 30\ \mathrm{ns}^{-1}$, $\gamma_2 = 10\ \mathrm{ns}^{-1}$ and the coupling coefficient $\kappa_r = 90\ \mathrm{ns}^{-1}$. Other parameters are identical for the master and slave lasers. It can be clearly seen that highest correlation coefficients are

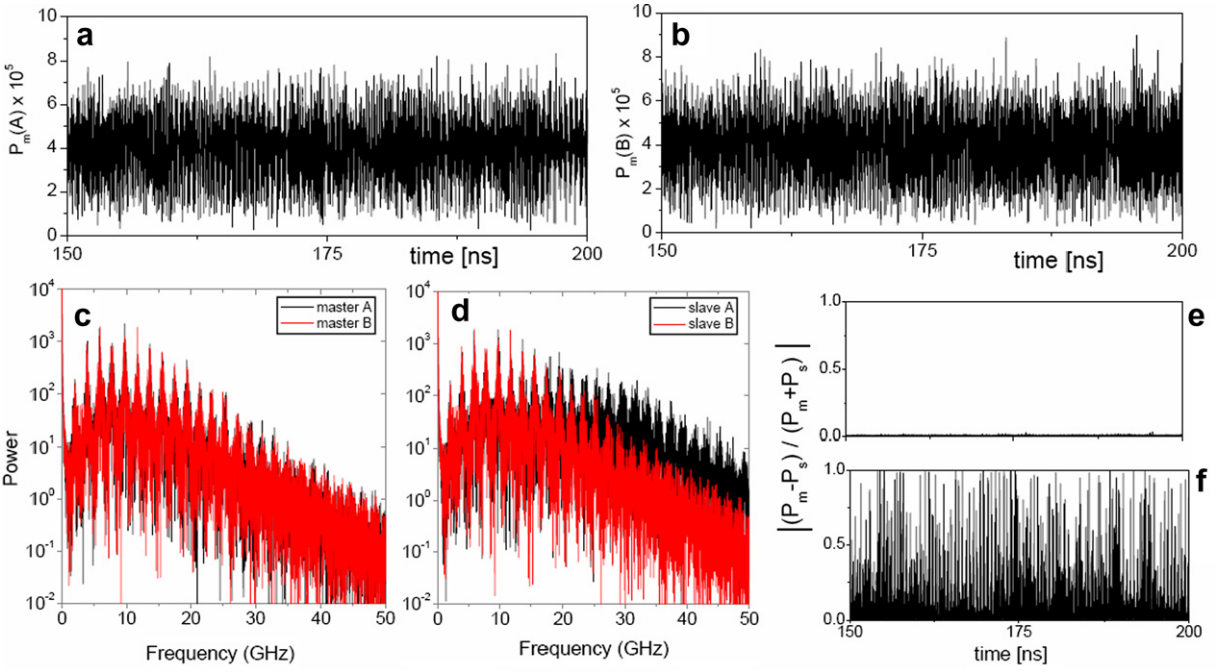

Fig. 8. Calculated pulse traces of the emitter laser at point A (a) and point B (b), shown in Fig. 7. Power spectra of the master (c) and slave (d) lasers. Panels (e) and (f) show the synchronization error for $\psi_m = \psi_s = 0.75$ rad and $\psi_m = 0, \psi_S = 0.75$ rad, respectively. Parameters are as in Fig. 7.

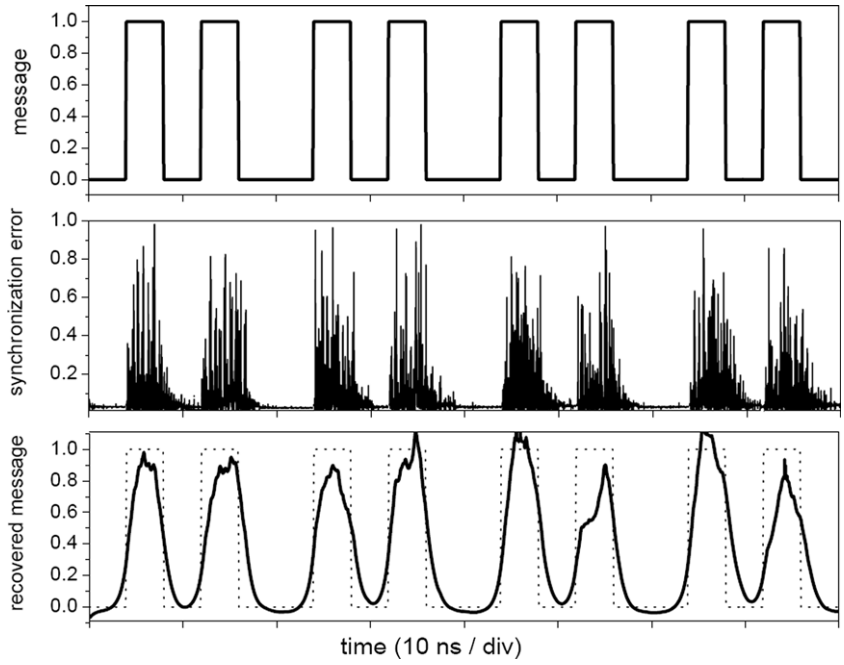

Fig. 9. On/off phase shift keying encoding and decoding of 0.25 Gb/s digital message. Top panel: encoded message. Central panel: decoded message represented by the synchronization error. Bottom panel: recovered message after filtering. The other parameters are as in Fig. 7.

achieved when the two phases coincide, i.e., $\psi_m = \psi_s$ while the correlation degrades when the phases start to be different. Points A and B in Fig. 7 correspond to the operating points that will be consider later for message encoding and decoding using OOPSK encryption. The point A is chosen to have high correlation while the point B (or B′) corresponds to a state with low correlation.

An important issue in chaos based communication systems is the security of proposed setup. Schemes such as chaos shift keying [28], chaos masking [33] and chaos modulation [7] require keeping the message amplitude small enough in order to avoid message recognition. In the OOPSK technique the message is codified by changing the feedback phase of the master laser without introducing significant changes in the time trace or spectrum of the emitted light [25,26]. In this setup the slave laser for which the feedback phase is kept constant, acts as a detector of the synchronization quality. When the feedback phases of the emitter and receiver coincide the correlation between the outputs of the two systems is high while it is low when the phases are different (as was shown in Fig. 7). In our scheme the phases ϕ of the COF branch are kept constant in both master and slave lasers while we study the phase shift keying method by varying the phase of the auxiliary branch. Fig. 8 shows the pulse traces of the master laser operating in the chaotic regime at the point A (a) and at point B (b). It can be clearly seen that both time traces remain similar to each other. Fig. 8c shows the power spectra of the time traces shown in Figs. 8a and b, while Fig. 8d shows the power spectra of the receiver system for the fixed phase $\psi_S = 0.75$ rad. The power spectra of the emitter system for the operating points *A* and *B*, as shown in Fig. 8c, remain almost unchanged. On the contrary the power spectrum of receiver laser changes, as shown in Fig. 8d, due to the coupling light that is uncorrelated with that generated by the receiver system. Figs. 8e and f show the synchronization error, defined as $|(P_m - P_s)/(P_m + P_s)|$, for different phases. For $\psi_m = \psi_s = 0.75$ rad (see Fig. 8e) the synchronization error is almost zero and the cross correlation coefficient approaches unity. On the other hand for $\psi_m = 0, \psi_S = 0.75$ rad synchronization degrades, as shown in Fig. 8f, and the synchronization error is very high.

Fig. 9 depicts the process of 0.25 Gbit/s message OOPSK encryption. On the top panel the digital message is shown. Fig. 9 (central panel) shows the synchronization error when the phase of the transmitter laser is changed from 0.75 rad (bit "0") to 0 (bit "1") i.e. from point A to point B of Fig. 7. Fig. 9 (bottom panel) shows that the message can be successfully recovered after a standard filtering process. Thus the proposed setup can distinctly increase the bit rate compared with that previously obtained in [26].

5. Summary and conclusions

In this paper we have studied the dynamics of a device composed by a semiconductor laser subject to a double cavity feedback. Main advantages of proposed scheme include the existence of two feedback strengths, two feedback phases and two delay times that can be controlled separately. The results presented in this paper show the following features: under appropriate conditions the setup shown in Fig. 1 is capable of generating a robust chaotic waveform; two of these devices can be synchronized when operating in the chaotic regime in a master-slave configuration if some parameters are properly matched; with this scheme a short resynchronization time, which is two orders of magnitude shorter than that of COF case, can be obtained; OOPSK encryption can be successfully applied at a rate of hundreds of Mbit/s. This means that such devices are promising candidates for fast on/off phase shift keying encryption.

Our investigations highlight new perspectives for the use of phase shift keying scheme in chaos based optical communication applications. We believe that our work provides a good basis for future studies and, in particular, provides some pointers for more detailed investigations of III–V integrated devices containing a phase modulation section and its practical application in chaos-based communication systems.

Acknowledgments

Authors acknowledge financial supports from the European Commission project Picasso IST-2005-34551 and Spanish MEC and FCDU projects TEC 2006-10009/MIC (PhoDECC) and FIS2007-60327 (FISICOS) and the Technical University of Moldova project 307b/s. IVE acknowledges the Russian President Stipend.

References

[1] A. Pikovsky, M. Rosenblum, J. Kurths, Synchronization A Universal Concept in Nonlinear Sciences, Cambridge University Press, Cambridge England, 2003.
[2] L.M. Pecora, T.L. Carrol, Phys. Rev. Lett. 64 (1990) 821.
[3] L.M. Pecora, T.L. Carrol, Phys. Rev. A 44 (1991) 2374.
[4] S. Donati, C.R. Mirasso (Eds.), Feature section on optical chaos and applications to cryptography, IEEE, J. Quantum Electron. 38 (9) (2002) 351 and references therein.
[5] L. Larger, J.-P.Goedgebeuer (Eds.), Special number on "Cryptography using Optical chaos" Comptes Rendus de l'Academie des Sciences-Dossier de Physique N. 5, 2004.
[6] A. Argyris, D. Syvridis, L. Larger, V. Annovazzi-Lodi, P. Colet, I. Fischer, J. García-Ojalvo, C.R. Mirasso, L. Pesquera, K. Alan Shore, Nature 438 (2005) 343.
[7] C.R. Mirasso, P. Colet, P. Garcia-Fernandez, IEEE Photon. Technol. Lett. 8 (1996) 299.
[8] V. Annovazzi-Lodi, S. Donati, A. Scire, IEEE J. Quantum Electron. 32 (1996) 953.
[9] S. Sivaprakasam, K.A. Shore, Opt. Lett. 24 (1999) 466.
[10] I. Fischer, Y. Liu, P. Davis, Phys. Rev. A 62 (1) (2000) 011801.
[11] A. Bogris, D.F. Kanakidis, A. Argyris, D. Syvridis, IEEE J. Quantum Electron. 41 (2005) 469.
[12] S. Tang, J.M. Liu, Opt. Lett. 26 (2001) 596.
[13] N. Gastaud, S. Poinsot, L. Larger, J.M. Merolla, M. Hanna, J.P. Goedgebuer, E. Malassenet, Electron. Lett. 40 (2004) 898.
[14] F.Y. Lin, M.C. Tsai, Opt. Express 15 (2007) 302.
[15] B. Krauskopf, D. Lenstra (Eds.), Fundamental Issues of Nonlinear Laser Dynamics, AIP Conference Proceedings 548, 2000.
[16] T. Perez, M. Radziunas, H.-J. Wünsche, C.R. Mirasso, F. Henneberger, IEEE Photon. Technol. Lett. 18 (2006) 2135.
[17] V.Z. Tronciu, H.-J. Wünsche, M. Wolfrum, M. Radziunas, Phys. Rev. E 73 (2006) 046205.
[18] V.Z. Tronciu, C.R. Mirasso, P.Colet, Chaos based communications using semi conductor lasers subject to feedback from an integrated double cavity, J. Phys. B: At Mol. Opt. Phys. 41 (2008), in press.
[19] S. Schikora, P. Hoevel, H-J. Wuensche, E. Schoell, F. Henneberger, Phys. Rev. Lett. 97 (2006) 213902.
[20] Yun Liu, Junjii. Ohtsubo, IEEE J. Quantum Electron. 33 (1997) 1163.
[21] F. Rogister, P. Mégret, O. Deparis, M. Blondel, T. Erneux, Opt. Lett. 24 (1999) 1218.
[22] F. Rogister, D.W. Sukow, A. Gavrielides, P. Mégret, O. Deparis, M. Blondel, Opt. Lett. 25 (2000) 808.
[23] F.R. Ruiz-Oliveras, A.N. Pisarchik, Opt. Express 14 (2006) 12859.
[24] M.W. Lee, P. Rees, K.A. Shore, S. Ortin, L. Pesquera, A. Valle, in: IEE Proceedings Optoelectronics 152, 2005, p. 97.
[25] M. Peil, T. Heil, I. Fischer, W. Elsässer, Phys. Rev. Lett. 88 (2002) 1741011.
[26] T. Heil, J. Mulet, I. Fischer, C.R. Mirasso, M. Peil, P. Colet, W. Elsäßer, IEEE J.Quantum Electron. QE-38 (2002) 1162.
[27] I. Fischer, Y. Liu, P. Davis, Phys. Rev. A 62 (2000) 011801 (R).
[28] A. Sanchez-Diaz, C.R. Mirasso, P. Colet, P. Garcia-Fernandez, IEEE J. Quantum Electron. 35 (1999) 292.
[29] G.D. VanWiggeren, R. Roy, Science 279 (1998) 1198.
[30] V. Annovazzi-Lodi, M. Benedetti, S. Merlo, T. Perez, P. Colet, C.R. Mirasso, Photon. Technol. Lett. 19 (2007) 76.
[31] R. Lang, K. Kobayashi, IEEE J. Quantum Electron. QE-16 (1980) 347.
[32] R. Vicente, T. Pérez, C.R. Mirasso, IEEE J. Quantum Electron. 38 (2002) 1197.
[33] C.R. Mirasso, "Application of Semiconductor lasers to secure Communications" Fundamental Issue of Nonlinear Laser Dynamics, B. Krauskopf, D. Lenstra (Ed.), 2000, 112.